Cortical Reorganization After Optical Alignment in Strabismic Patients Outside of Critical Period

Yiru Huang,[1] Zitian Liu,[1] Mingqin Wang,[1] Le Gao,[1] Yanyan Wu,[1] Jingyi Hu,[1] Zhenyu Zhang,[2,3] Fang-Fang Yan,[2,3] Daming Deng,[1] Chang-Bing Huang,[2,3] and Minbin Yu[1]

[1]State Key Laboratory of Ophthalmology, Zhongshan Ophthalmic Center, Sun Yat-Sen University, Guangdong Provincial Key Laboratory of Ophthalmology and Visual Science, Guangdong Provincial Clinical Research Center for Ocular Diseases, Guangzhou, Guangdong, China
[2]Key Laboratory of Behavioral Science, Institute of Psychology, Chinese Academy of Sciences (CAS), Beijing, China
[3]Department of Psychology, University of Chinese Academy of Sciences, Beijing, China

Correspondence: Minbin Yu, State Key Laboratory of Ophthalmology, Guangdong Provincial Key Lab of Ophthalmology and Visual Science, Zhongshan Ophthalmic Center, Sun Yat-Sen University, Guangzhou, Guangdong, China; yuminbin@mail.sysu.edu.cn. Chang-Bing Huang, Institute of Psychology, Chinese Academy of Sciences (CAS), Beijing, China; Department of Psychology, University of Chinese Academy of Sciences, Beijing, China; huangcb@psych.ac.cn.

YH and ZL contributed equally to the work presented here and share senior authorship.

Received: March 22, 2023
Accepted: July 17, 2023
Published: August 3, 2023

Citation: Huang Y, Liu Z, Wang M, et al. Cortical reorganization after optical alignment in strabismic patients outside of critical period. *Invest Ophthalmol Vis Sci.* 2023;64(11):5. https://doi.org/10.1167/iovs.64.11.5

Purpose. To measure visual crowding, an essential bottleneck on object recognition and reliable psychophysical index of cortex organization, in older children and adults with horizontal concomitant strabismus before and after strabismus surgery.

Methods. Using real-time eye tracking to ensure gaze-contingent display, we examined the peripheral visual crowding effects in older children and adults with horizontal concomitant strabismus but without amblyopia before and after strabismus surgery. Patients were asked to discriminate the orientation of the central tumbling E target letter with flankers arranged along the radial or tangential axis in the nasal or temporal hemifield at different eccentricities (5° or 10°). The critical spacing value, which is the minimum space between the target and the flankers required for correct discrimination, was obtained for comparisons before and after strabismus surgery.

Results. Twelve individuals with exotropia (6 males, 21.75 ± 7.29 years, mean ± SD) and 15 individuals with esotropia (6 males, 24.13 ± 5.96 years) participated in this study. We found that strabismic individuals showed significantly larger critical spacing with nasotemporal asymmetry along the radial axis that related to the strabismus pattern, with exotropes exhibiting stronger temporal field crowding and esotropes exhibiting stronger nasal field crowding before surgical alignment. After surgery, the critical spacing was reduced and rebalanced between the nasal and temporal hemifields. Furthermore, the postoperative recovery of stereopsis was associated with the extent of nasotemporal balance of critical spacing.

Conclusions. We find that optical realignment (i.e., strabismus surgery) can normalize the enlarged visual crowding effects, a reliable psychophysical index of cortical organization, in the peripheral visual field of older children and adults with strabismus and rebalance the nasotemporal asymmetry of crowding, promoting the recovery of postoperative stereopsis. Our results indicated a potential of experience-dependent cortical organization after axial alignment even for individuals who are out of the critical period of visual development, illuminating the capacity and limitations of optics on sensory plasticity and emphasizing the importance of ocular correction for clinical practice.

Keywords: visual crowding, strabismus, axial alignment, cortical reorganization

How we "see" the world is one of the fundamental challenges in brain science, understanding of which requires insights into both optical and cortical elements involved in visual perception. Setting fundamental constraints over retinal image quality, the eye's optics drives normal maturation of visual cortical processing.[1,2] For binocular creatures, one of the characteristic optics is that we are long-adapted to a two-eye visual mode in which two eyes coordinate in an aligned fashion to form a unifying three-dimensional representation of the external world.[3] If the visual axes of two eyes are misaligned, retinal correspondence is disrupted, and strabismus may develop.[4] Without timely and appropriate treatment, strabismus may lead to functional changes and abnormal functional connectivity of the visual cortex,[5–7] resulting in a variety of visual deficits (e.g., defective stereopsis, increased fixation instability, interocular suppression, abnormal retinal correspondence, and even amblyopia).[8–10] Following the doctrine that cortical plasticity will diminish after the critical period, the common clinical practice for strabismus is thus to correct the visual axis in early childhood.[11] By measuring visual crowding, a reliable psychophysical index of cortical organization, here we show that surgical alignment of the visual axis in older children and adults with strabismus but without amblyopia

also leads to cortical reorganization, adding new insights on the capacity and limits of the eye's optics on sensory plasticity.

Visual crowding characterizes humans' inefficiency in identifying objects in clutter but cannot simply be explained by reduced visual acuity or contrast sensitivity at a given retinal location.[12–15] The magnitude of the crowding effects, usually indexed by critical spacing (i.e., the minimum spacing between a target and flankers required for reliable target identification), expands with increasing retinal eccentricity.[16–19] It has been reported that visual crowding reflects the neuroanatomic limits of cortical processing of object recognition,[14,20] with the extent of critical spacing negatively correlated with the cortical magnification factor.[21–24] Psychophysical measurement of visual crowding has thus been applied to characterize cortical plasticity following long-term adaptation to retinal lesion or central vision deprivation such as age-related macular degeneration,[17] glaucoma,[25,26] and amblyopia.[27] On the other hand, as the common way to restore ocular alignment, empirical observations have shown that even in adults, strabismus surgery may also lead to the improvement or recovery of binocular functions.[28–31] One possible conjecture is that restoring coordination between the signals from the two eyes probably results in cortical reorganization of intracortical neuronal connections.[32]

In the present study, we used real-time eye tracking to ensure gaze-contingent display of the target and flankers at four different retinal locations and measured the critical spacing value in 12 exotropes and 15 esotropes before and after surgical operation to assess whether axial alignment could induce cortical reorganization in older children and adults with strabismus. We found that before surgery, strabismic individuals manifested significantly larger critical spacing with field- and axis-specific patterns along only the radial axis, with exotropes exhibiting stronger temporal hemifield crowding and esotropes exhibiting stronger nasal hemifield crowding, which is consistent with our previous study,[33] even though the individuals of these two studies were not from the same group. Interestingly, the critical spacing was reduced and rebalanced between the nasal and the temporal hemifields 3 months after surgical correction of ocular misalignment, which correlated with postoperative stereopsis recovery. Overall, our results revealed that the visual cortex could be reorganized in response to correction of visual alignment even in humans outside of the typical critical period.

Methods

Patients

Individuals with horizontal concomitant strabismus but without amblyopia were recruited through the Zhongshan Ophthalmic Center, Guangzhou, China. Twelve individuals with exotropia (6 men, 21.75 ± 7.29 years, mean ± SD) and 15 individuals with esotropia (6 men, 24.13 ± 5.96 years) participated in this study. This study followed the principles of the Declaration of Helsinki and was approved by the Institutional Review Board of Zhongshan Ophthalmic Center, Sun Yat-sen University. After explaining the purpose, procedures, risks, and benefits of this study, informed consents were obtained from patients or their parents/legal guardians.

All individuals underwent comprehensive eye examinations before and 3 months after strabismus surgery, including a review of medical history, cycloplegic refraction and determination of the best-corrected distance visual acuity, examination of eye movements, alternate prism cover tests at near and distance fixations, slit-lamp examination, funduscopic examination, and stereoacuity test (Vision Assessment Corporation Co., Elk Grove Village, IL, USA).

Horizontal concomitant strabismus is defined as a horizontal deviation of the visual axis and an identical angle of deviation of the squinting eye relative to the other eye, regardless of the direction of the gaze.[34–36] All individuals reported alternating strabismus with shifted fixation between their eyes and ocular deviation at both near and distant. According to the Preferred Practice Patterns of the American Academy of Ophthalmology,[37] individuals who had clinically significant refractive error were instructed to wear spectacles for at least 3 months before the experiment, and only those who had normal or corrected-to-normal visual acuity (0.00 logMAR or better) after refractive correction were included in this study. All individuals had a history of strabismus since early childhood (3.33 ± 3.56 years old, mean ± SD) and had never received strabismus surgery before. All individuals had no history of vertical, paralytic, or restrictive strabismus; accommodative esotropia; acute concomitant esotropia; nystagmus; or a history of ocular surgery or prism correction. Individuals with any neurologic disorders or systemic diseases were also excluded.

All individuals underwent strabismus surgery (rectus shortening and/or recession) to recover axial alignment after the preoperative measurement, and a postoperative measurement was performed 3 months after the surgery. Successful postoperative axial alignment is considered less than 10 prism diopters.[34] Clinical characteristics of each individual are summarized in Table.

Apparatus

Experimental stimuli were programmed with MATLAB R2018a (MathWorks, Inc., Natick, MA, USA) using the Psychtoolbox extension (Version 3.0.14).[38] All stimuli were presented on a gamma-corrected liquid crystal display screen with a resolution of 1920 × 1080, a refresh rate of 144 Hz, and a uniform gray background of 54 cd/m^2. Patients were seated at an eye-to-screen distance of 57 cm with a chin-and-forehead rest to limit head movements.

Stimuli

The stimuli consisted of a single black tumbling E in the visual acuity test and a trigram of black tumbling Es with the middle one as the target in the crowding test. Patients were asked to report the orientation (left, right, up, or down) of the target tumbling E by pressing the appropriate key on the keyboard. The trigrams were arranged along the radial or tangential axis at an eccentricity of 5° or 10° in the nasal or temporal hemifield, resulting in eight testing conditions appearing randomly (see Fig. 1A).

Eye Movement Recording

A high-resolution infrared-emitting video-based eye tracker sampled at 1000 Hz (EyeLink 1000; SR Research, Ottawa, Canada) was used, with a maximum spatial resolution of 0.02°, to continuously monitor patients' eye positions. We performed and repeated a standard five-point calibration and validation sequence at the beginning of every test until the validation error was smaller than 1° on average.[39] The

Table. Clinical Characteristics of Strabismic Individuals

Patient	Age/Sex	VA, DE logMAR	VA, FE logMAR	Refraction DE	Refraction FE	Duration of Strabismus, y	Preoperative Alignment (Prism Diopters)	Preoperative Stereoacuity (Arcsecs)	Preoperative Retinal Correspondence Test	Postoperative Alignment (Prism Diopters)	Postoperative Stereoacuity (Arcsecs)	Postoperative Retinal Correspondence Test
EXO1	28/M	−0.10	−0.10	+1.75	+1.25/−0.5 × 10	18	XT 60	None	MS	XT 5	50	ARC
EXO2	25/M	0.00	0.00	+1.25/−1.0 × 5	+0.25/−0.75 × 5	25	XT 45	None	MS	Ortho	100	ARC
EXO3	14/F	0.00	0.00	−3.5/−2.25 × 170	−3.5/−1.5 × 180	12	XT 45	None	MS	Ortho	20	NRC
EXO4	17/M	0.00	0.00	−6.0/−0.5 × 100	+0.75/−2.25 × 125	14	XT 45	None	NRC	Ortho	50	NRC
EXO5	13/F	0.00	0.00	−2.5/−0.5 × 175	+0.5/−0.5 × 160	13	XT 55	None	MS	Ortho	40	NRC
EXO6	18/F	0.00	−0.10	−1.0	PL	13	XT 55	None	MS	Ortho	400	NRC
EXO7	20/F	0.00	0.00	−2.75	PL	18	XT 35	None	MS	Ortho	40	ARC
EXO8	13/M	0.00	0.00	+1.75/−1.50 × 165	+1.0/−1.25 × 180	9	XT 45	None	MS	Ortho	50	NRC
EXO9	22/F	0.00	−0.05	PL	−2.75	16	XT 60	None	MS	XT 10	None	ARC
EXO10	36/F	0.00	0.00	−0.5/−1.0 × 80	+0.5/−0.5 × 105	30	XT 45	None	MS	Ortho	25	ARC
EXO11	25/M	0.00	0.00	+1.00	+0.25	25	XT 60	None	MS	XT 8	None	ARC
EXO12	30/M	0.00	0.00	PL	−1.0	25	XT 35	None	MS	X 3	None	MS
ESO1	28/F	−0.05	0.00	−5.00	−2.00/−0.75 × 135	25	ET 60	None	MS	ET 10	None	MS
ESO2	28/F	0.00	0.00	−4.50/−1.25 × 170	−6.50/−0.75 × 167	28	ET 35	None	MS	Ortho	None	MS
ESO3	20/M	0.00	0.00	−9.50/−1.00 × 180	−10.00/−0.75 × 180	19	ET 55	None	MS	ET 5	None	ARC
ESO4	19/F	0.00	0.00	+0.5	−0.50/−0.50 × 95	19	ET 25	None	MS	ET 8	500	NRC
ESO5	14/M	−0.05	0.00	+6.75/−1.25 × 180	+5.50/−1.25 × 180	10	ET 35	None	MS	ET 10	None	MS
ESO6	30/M	0.00	0.00	+1.25/−0.5 × 10	+1.5/−1.5 × 20	25	ET 80	None	MS	Ortho	100	NRC
ESO7	15/M	−0.05	0.00	+6.50/−1.00 × 175	+4.50/−0.75 × 180	12	ET 55	None	MS	Ortho	160	NRC
ESO8	25/F	0.00	0.00	+0.25	−0.5 × 155	20	ET 25	None	MS	E 3	100	NRC
ESO9	18/M	0.00	0.00	−2.25/−0.5 × 170	−2.5/−0.5 × 20	18	ET 45	None	MS	ET 5	200	ARC
ESO10	26/F	0.00	0.00	−4.0/−0.5 × 170	−4.5	10	ET 60	None	MS	Ortho	None	MS
ESO11	33/F	0.00	0.00	−0.25/−0.5 × 145	−0.5/−0.5 × 160	30	ET 45	None	MS	E 3	None	MS
ESO12	26/F	0.00	−0.10	−4.50/−1.0 × 85	−1.25/−0.5 × 85	26	ET 45	None	MS	ET 10	None	MS
ESO13	24/F	0.00	0.00	+6.50/−1.50 × 180	+5.50/−1.25 × 180	20	ET 55	None	MS	Ortho	None	MS
ESO14	23/M	0.00	0.00	+3.75/−2.25 × 20	+1.00/−0.5 × 5	23	ET 80	None	MS	Ortho	None	MS
ESO15	33/F	0.00	0.00	+3.5/−0.5 × 55	+2.50/−0.5 × 120	30	ET 80	None	MS	Ortho	160	NRC

Retinal correspondence test: Synoptophore test, Bagolini test.

ARC, anomalous retinal correspondence; E, esophoria; ESO/ET, esotropia; EXO/XT, exotropia; DE, deviated eye; FE, fixating eye; MS, monocular suppression; NRC, normal retinal correspondence; Ortho, orthophoria; PL, plano; X, exophoria.

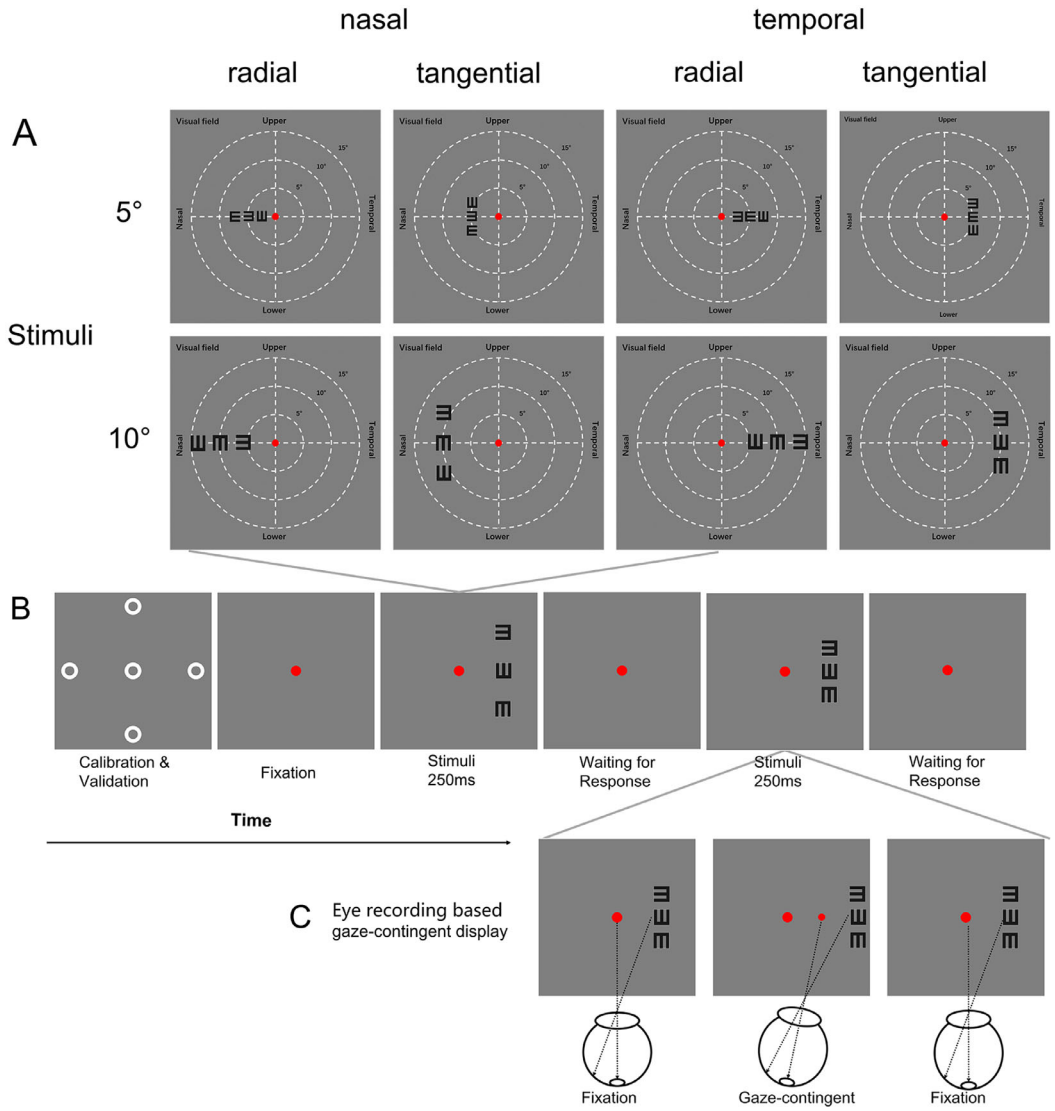

Figure 1. Schematic description of the visual crowding test. (**A**) Stimuli used in the visual crowding test. The stimuli consisted of a target tumbling E flanked by two tumbling Es arranged on both sides of the target along the radial or tangential axis. Critical spacing value was measured in the nasal or temporal hemifield at the eccentricities of 5° or 10°, respectively, leading to a total of eight kinds of testing stimuli (2 axes × 2 visual fields × 2 eccentricities). (**B**) Time course of the crowding test. After a standard five-point calibration and validation, the trial began with a central red fixation point presenting throughout the test. The stimuli appeared randomly for 250 ms, followed by an interstimulus interval for patients to respond without time limitation. After the response, there was a brief pause of 1 second and then the next trial started. A three-down, one-up staircase was adopted to track the spacing between the center of the target and the center of the flankers. (**C**) Eye recording–based gaze-contingent display. A video-based eye tracker was used to continuously monitor patients' eye positions, with a gaze-contingent paradigm to ensure the display of the target and flankers in the specific visual field locations. Once the eye tracker detected patients' involuntary eye movement toward the target letter, the program would move the target and flank letters at an identical direction and distance to offset the involuntary eye movement.

average gaze error was 0.5°, ranging from 0.1° to 1°. An eye recording–based gaze-contingent display was used to ensure the display of the target and flankers in the specific visual field locations (see Fig. 1C). Once the eye tracker detected the involuntary eye movement of the patient to the target letter, the program would move the target and flank letters at the identical direction and distance to offset the involuntary eye movement. During the whole test, a chin-and-forehead rest was used to minimize head movements and trial-to-trial variability in the estimate of gaze position. A good fixation was defined as a stable fixation for at least 250 ms and positions not exceeding 0.5° in any direction.[39] Trials that failed to meet the requirements of good fixation were repeated until the requirements were met.

Design

The test was monocular with the untested eye covered by a black patch. To isolate the effect of crowding from that of simply missing the target, we conducted a visual acuity test at first to obtain the minimum letter size visible to the patients and ensured that they could see the target in isolation clearly. In the following crowding test, the initial letter size was set to 1.5 times the minimum letter size estimated

from the visual acuity test, and the initial spacing between the center of the target and the center of the flankers was 0.75 times the eccentricity.[40] Critical spacing of crowding across the radial or tangential axis in the nasal or temporal visual fields was measured at two eccentricities (5° and 10°), leading to a total of eight crowding measurements (2 axes × 2 visual fields × 2 eccentricities). All individuals completed tests with their nondominant eye (determined with the Mile's test)[41,42] in both the preoperation and the postoperation measurements.

Procedure

After completing a standard five-point calibration and validation[43] to provide the horizontal and vertical position measurement of the test eye, patients were instructed to fixate on the central red point. Stimuli were briefly presented for 250 ms, and eight different testing conditions were randomly interleaved. Patients were asked to identify the orientation of the target tumbling E by pressing the corresponding key on a computer keyboard. After each response, there was a short pause of 1 second, and then the next trial began (see Fig. 1B). The distance between the center of the target and the center of the flankers was tracked using a three-down, one-up staircase with a 10% step size,[44,45] in which three consecutive correct discriminations of the orientation of the target tumbling E led to a decrease of the center-to-center distance between the target and the flankers by 10% (i.e., $Distance_{t+1} = Distance_t \times 90\%$), while an incorrect discrimination led to a 10% increase in the distance (i.e., $Distance_{t+1} = Distance_t \times 110\%$). After six reversals, the staircase procedure ended and the average spacing of the last four reversals was regarded as the critical spacing value (i.e., the space between the center of the target and the center of the flankers required for 79.4% correct identification). The same methods of staircase and reversal were used to calculate the visual acuity threshold in the visual acuity test.

Before the test, the patients were explained the task and given an opportunity to practice for 10 minutes. Patients who did not complete the test well or who did not maintain good fixation stability during the test were excluded. We recruited a total of 15 exotropes and 15 esotropes, and 3 exotropes were excluded due to poor fixation. As a result, 12 exotropes and 15 esotropes successfully completed both the preoperative and postoperative measurements and were included in the final analysis.

Statistical Analysis

To reduce the influence of eccentricity,[46] we first normalized the critical spacing by dividing these values by the measured eccentricity to obtain the normalized critical spacing (NCS). A mixed repeated-measures ANOVA with axis (radial or tangential), eccentricity (5° or 10°), visual field (nasal or temporal), and operation (preoperative or postoperative) as the within-subject factors and group (exotropia or esotropia) as the between-subject factor was carried out. Since we found that the NCS of each group was comparable in both eccentricities (5° and 10°; see Supplementary Table S1), we combined the NCS measured at the same visual field across two eccentricities for the following analysis.

The combined NCS was analyzed by repeated-measures ANOVA, with within-subject factors of axis (radial or tangential), visual field (nasal or temporal), and operation (preoperative or postoperative) for exotropia and esotropia groups separately. The pairwise post hoc comparisons (with Bonferroni correction) were performed to compare the NCS before and after the operation in each group.

Horizontal concomitant strabismus turns its visual axis to the nasal (e.g., esotropia) or temporal (e.g., exotropia) field of vision. In order to better describe the crowding effects across different visual fields, we calculated the ratio of the NCS between the nasal and the temporal hemifields (or critical spacing ratio, CSR) as $(NCS_{nas} - NCS_{temp}) / (NCS_{nas} + NCS_{temp})$. CSR values of <0, 0, and >0 indicate greater crowding effects in the temporal hemifield, symmetrical crowding effects across visual fields, and greater crowding effects in the nasal hemifield, respectively.[47] The CSR was analyzed by repeated-measures ANOVA with within-subject factors of axis (radial or tangential) and operation (preoperative or postoperative) and the pairwise post hoc comparisons (with Bonferroni correction) to examine whether the CSR differed significantly before and after strabismus surgery in each group. In addition, a single-sample *t*-test was conducted to examine whether the CSR was significantly different from zero.

To figure out whether strabismus surgery could improve the patient's fixation stability and thus reduce the visual crowding effects, we analyzed the eye positions using MATLAB (MathWorks) and quantified the fixation stability by calculating the bivariate contour ellipse area (BCEA) using the following equation[48–50]:

$$\mathbf{BCEA} = \pi \mathbf{X}^2 \sigma_x \sigma_y \sqrt{1 - \boldsymbol{p}^2}$$

where $\mathbf{X}^2$ is a chi-square variable with two degrees of freedom; σ_x and σ_y are the standard deviation of eye position in the horizontal and vertical meridians, respectively; and $\boldsymbol{p}$ is the correlation coefficient of the moment of the Pearson product of the horizontal and vertical eye positions. The area of 68% BCEA was used in this study as a quantitative measure of fixation instability. It refers to the area in squared degrees (deg^2) of the ellipse around the stimulus containing most of the fixation points. Therefore, the smaller the BCEA value is, the more stable the gaze is. A $\log_{10}$ transformation was used to normalize the resulting BCEA values (logBCEA). We also analyzed the distribution of fixation points in the nasal and temporal visual fields during the test to explore the influence of oculomotor bias on the detection of crowding effects.

Data are reported as mean ± SD unless otherwise noted. All statistical analyses were performed using IBM SPSS Statistics Version 25 (IBM, Armonk, NY, USA) and JASP 0.14.1.0 (https://jasp-stats.org), with $P < 0.05$ as the criterion for statistical significance.

Results

With comprehensive eye examinations, 12 individuals with exotropia (6 males, 21.75 ± 7.29 years, mean ± SD) and 15 individuals with esotropia (6 males, 24.13 ± 5.96 years) were recruited and psychophysically tested visual crowding before and 3 months after strabismus surgery. Using a real-time eye tracker and gaze-contingent display paradigm, the crowding test was performed to measure the critical spacing (i.e., the center-to-center spacing between the center target and flankers that corresponds to 79.4% correct identification) across radial and tangential axes in the nasal and

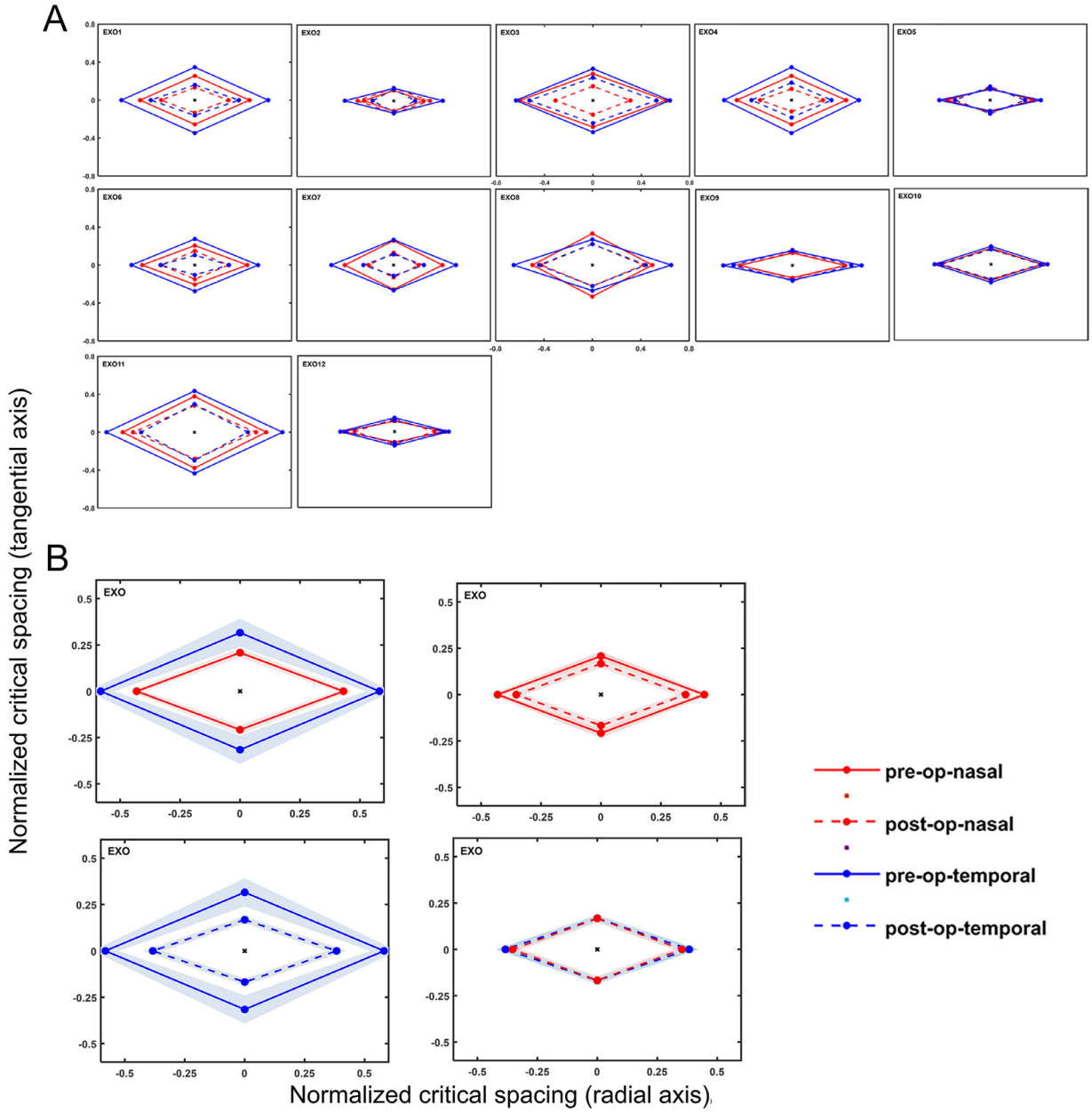

Figure 2. Crowding zones mapped from the normalized critical spacing across the nasal and temporal hemifields for 12 exotropes before and after surgery. For each hemifield, the size of the crowding zone was shown for radial and tangential axes. The *solid red line* represents the crowding zone in the nasal hemifield before surgery. The *solid blue line* represents the crowding zone in the temporal hemifield before surgery. The *dotted red line* represents the crowding zone in the nasal hemifield after surgery. The *dotted blue line* represents the crowding zone in the temporal hemifield after surgery (see color legend). (**A**) The crowding zone of each exotropia individual. (**B**) The average crowding zone of the exotropes groups ($n = 12$). The *light shaded regions* indicate the SEM across individuals.

temporal visual fields at two eccentricities (5° and 10°), leading to a total of eight crowding measurements (2 axes × 2 visual fields × 2 eccentricities).

To reduce the influence of eccentricity,[46] we first normalized the critical spacing by dividing the values by the eccentricity at which they were measured to get the NCS. A mixed repeated-measures ANOVA revealed that the NCS varied significantly with surgical operation ($F_{1, 25} = 24.51$; $P < 0.001$) and axis ($F_{1, 25} = 253.07$; $P < 0.001$) but not hemifield ($F_{1, 25} = 0.92$; $P = 0.346$), eccentricities ($F_{1, 25} = 1.64$; $P = 0.213$), and groups ($F_{1, 25} = 0.14$; $P = 0.716$; see Supplementary Table S1 for details). Since the interaction of eccentricity and group was also nonsignificant ($F_{1, 25} = 2.12$; $P = 0.158$), our results indicated that the NCS was comparable across the two eccentricities in esotropia and exotropia groups. Mean NCS across eccentricities (i.e., average of the data of 5° and 10° eccentricities in the same hemifield locations) was thus used in the following analysis.

Peripheral Visual Crowding Effects in Older Children and Adults With Exotropia Before and After Surgical Alignment

Crowding zones mapped from the NCS across nasal and temporal hemifields for 12 exotropes (EXO) before and after

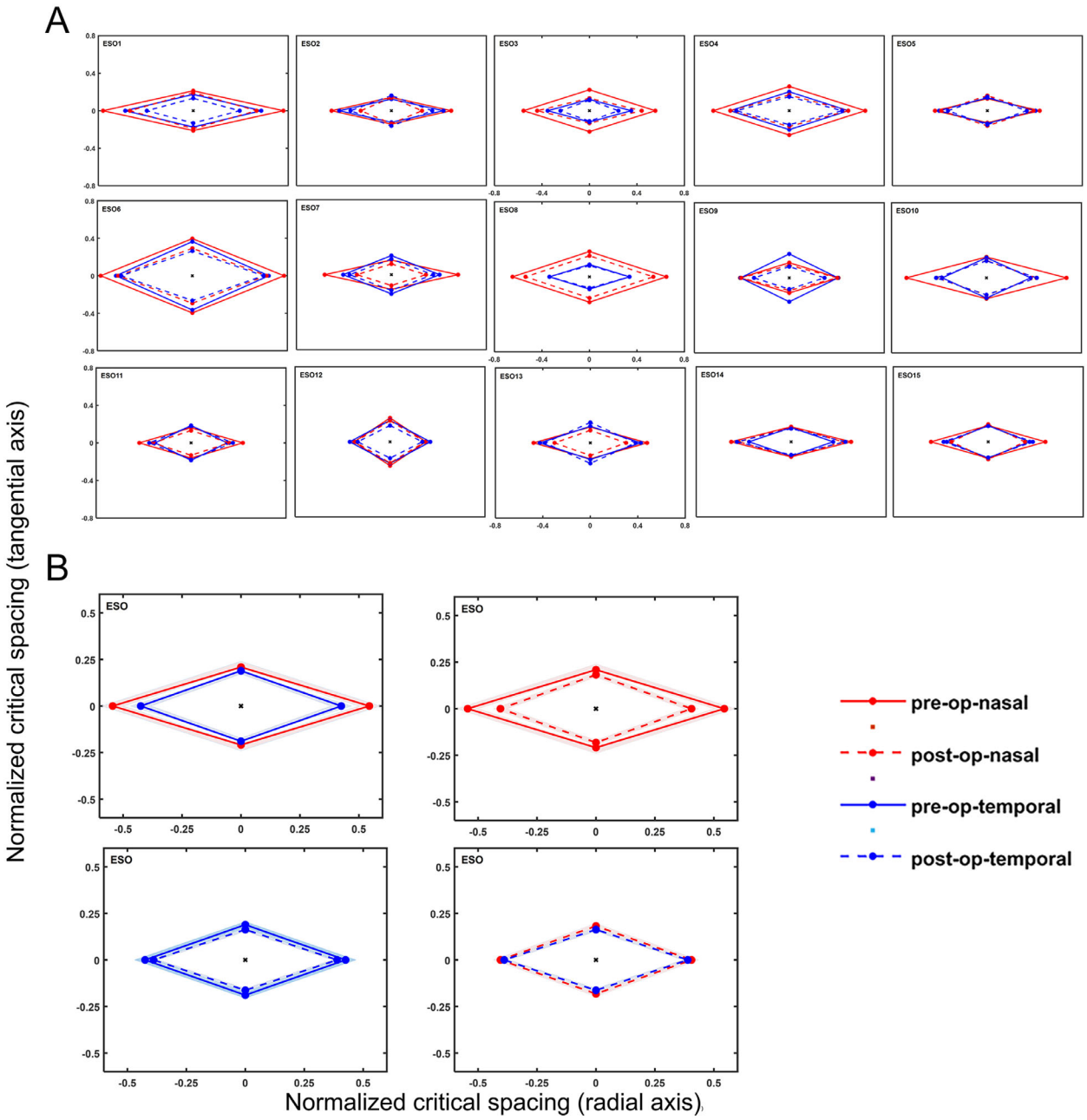

Figure 3. Crowding zones mapped from the normalized critical spacing across the nasal and temporal hemifields for 15 esotropes before and after surgery. For each hemifield, the size of crowding zone was shown for radial and tangential axes. The *solid red line* represents the crowding zone in the nasal hemifield before surgery. The *solid blue line* represents the crowding zone in the temporal hemifield before surgery. The *dotted red line* represents the crowding zone in the nasal hemifield after surgery. The *dotted blue line* represents the crowding zone in the temporal hemifield after surgery (see color legend). (**A**) The crowding zone of each esotropia individual. (**B**) The average crowding zone of the esotropes groups ($n = 15$). The *light shaded regions* indicate the SEM across individuals.

surgery are plotted in Figure 2. Before surgery, the average NCS of exotropes was 0.43 ± 0.09 at the radial axis and 0.21 ± 0.08 at the tangential axis in the nasal hemifield, as well as 0.58 ± 0.18 and 0.32 ± 0.26, respectively, in the temporal hemifield. After surgical alignment, the NCS decreased to 0.35 ± 0.11 at the radial axis and 0.17 ± 0.07 at the tangential axis in the nasal hemifield, as well as 0.38 ± 0.13 at the radial axis and 0.17 ± 0.06 at the tangential axis in the temporal hemifield. When a repeated-measures ANOVA was performed, the effects of surgical operation ($F_{1,\ 11} = 13.94$; $P = 0.003$), hemifield ($F_{1,\ 11} = 6.77$; $P = 0.025$), and axis ($F_{1,\ 11} = 214.58$; $P < 0.001$; see Supplementary Table S2 and Supplementary Table S4 for details) were significant. A pairwise post hoc comparison (with Bonferroni correction) showed a significant difference in the NCS before and after operation in the temporal hemifield (radial: $t = 4.80$, $P < 0.001$; tangential: $t = 3.58$, $P = 0.038$) but not in the nasal hemifield (radial: $t = 1.91$, $P = 1.00$; tangential: $t = 0.99$, $P = 1.00$). Moreover, the NCS along the radial axis was significantly larger in the temporal hemifield, as

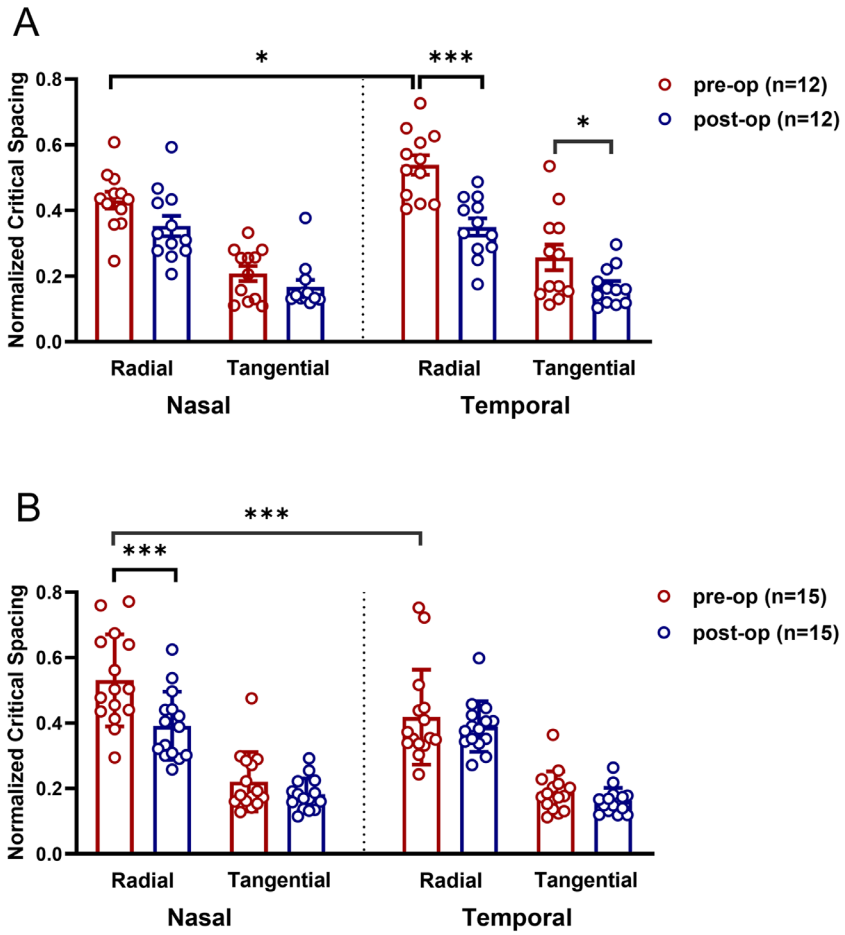

Figure 4. (**A**) The normalized critical spacing across different hemifields and axes for exotropes before and after surgery. (**B**) The normalized critical spacing across different hemifields and axes for esotropes before and after surgery. Higher values on the y-axes signify stronger crowding effects. Statistically significant difference: *$P < 0.05$, ***$P < 0.001$.

opposed to the nasal hemifield before the surgery (nasal versus temporal: $t = 3.90$, $P = 0.015$). However, no significant difference in the NCS between the nasal and temporal hemifields along the radial axis was found after surgery ($t = 0.79$, $P = 1.00$; Fig. 4A).

In short, similar to our previous study, in which nasotemporal symmetry crowding effects of normal individuals and nasotemporal asymmetry crowding effects of strabismic patients were reported,[33] we found that exotropes manifested stronger peripheral visual crowding effects in the temporal hemifield (i.e., the deviating direction of fixation), and surgical correction of ocular position significantly reduced and rebalanced the crowding effects.

Peripheral Visual Crowding Effects in Older Children and Adults With Esotropia Before and After Surgical Alignment

Crowding zones mapped from the NCS across the nasal and temporal hemifields for 15 esotropes (ESO) before and after surgery are plotted in Figure 3. Before surgery, the average NCS of esotropes was 0.54 ± 0.17 at the radial axis and 0.21 ± 0.12 at the tangential axis in the nasal hemifield, as well as 0.43 ± 0.17 and 0.19 ± 0.06, respectively, in the temporal hemifield. After surgical alignment, the NCS reduced to 0.41 ± 0.11 at the radial axis and 0.18 ± 0.05 at the tangential axis in the nasal hemifield, as well as 0.39 ± 0.08 at the radial axis and 0.16 ± 0.04 at the tangential axis in the temporal hemifield. A repeated-measures ANOVA revealed that the effects of surgical operation ($F_{1, 14} = 8.96$; $P = 0.010$), hemifield ($F_{1, 14} = 8.77$; $P = 0.010$), and axis ($F_{1, 14} = 114.29$; $P < 0.001$; see Supplementary Table S3 and Supplementary Table S5 for details) were significant. A pairwise post hoc comparison (with Bonferroni correction) showed the NCS after surgery was significantly decreased compared with the corresponding NCS before surgery in the nasal hemifield along the radial axis ($t = 5.04$, $P < 0.001$) but not along the tangential axis ($t = 0.96$, $P = 1.00$) or in the temporal hemifield (radial axis: $t = 1.28$, $P = 1.00$; tangential axis: $t = 0.95$, $P = 1.00$). Besides, consistent with our previous report,[33] the NCS in the nasal hemifield was significantly larger than that in the temporal hemifield along only the radial axis before surgery (nasal versus temporal: $t = 5.55$, $P < 0.001$), but no difference of the NCS was found between the nasal and temporal hemifields after surgery (radial axis: $t = 0.72$, $P = 1.00$; tangential axis: $t = 0.91$, $P = 1.00$; Fig. 4B).

In general, we found that esotropes manifested stronger peripheral visual crowding effects in the nasal hemifield (i.e., the deviating direction of fixation), which could also be significantly reduced and became relatively nasotemporally balanced after surgical correction.

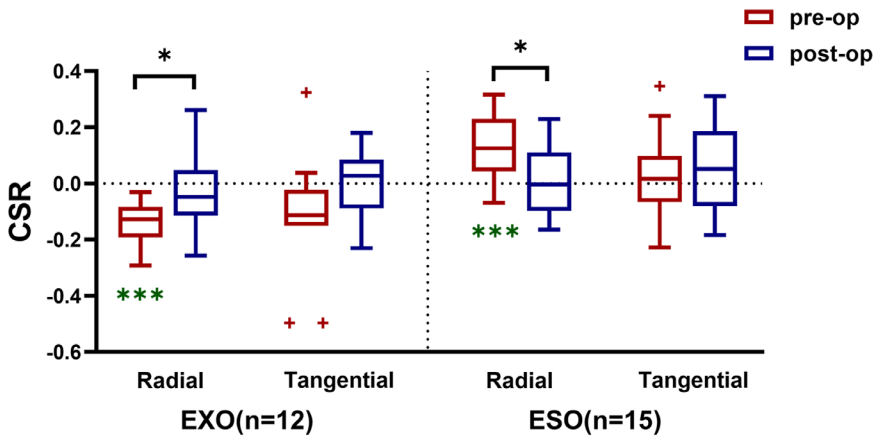

Figure 5. Boxplots of the CSR of exotropia and esotropia groups before and after surgery. The *solid line* within each *box* represents the median. The *box* represents the interquartile range (IQR) of the data (75th to the 25th percentile, e.g., Q3–Q1), and the data points with *red crosses* represent outliers. Outliers were defined as values less than Q1 – 1.5 × IQR or greater than Q3 + 1.5 × IQR. The *gray dashed line* indicates a CSR of 0. A CSR of <0, 0, and >0 indicates greater crowding effects in the temporal hemifield, symmetrical crowding effects across visual fields, and greater crowding effects in the nasal hemifield, respectively. To avoid interference with the results, outliers were excluded from the statistical analysis. A pairwise post hoc comparison (with Bonferroni correction) was performed to test if the CSR differed significantly before and after strabismus surgery, and *black asterisks* above indicate a statistically significant difference: *$P < 0.05$. A single-sample *t*-test was conducted to examine whether the CSR was significantly different from zero, and *green asterisks* below indicate significant differences from zero: ***$P < 0.001$.

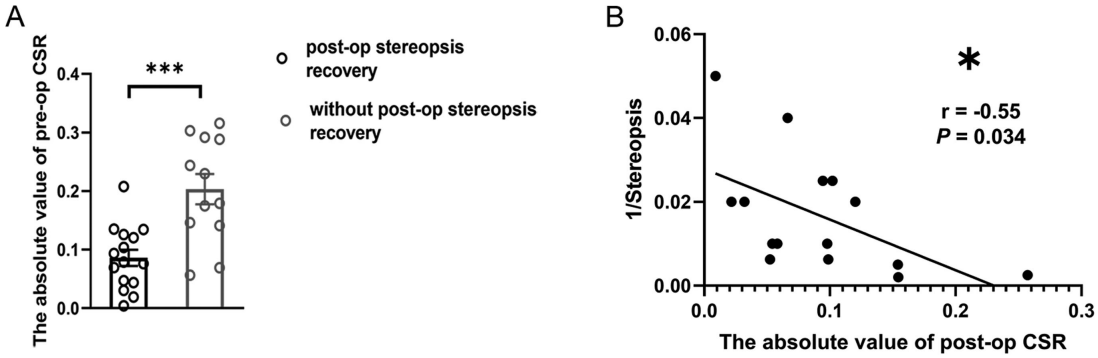

Figure 6. (**A**) Comparisons of the absolute value of the preoperative CSR between individuals with postoperative stereopsis recovery ($n = 15$) and individuals without postoperative stereopsis recovery ($n = 12$). *Error bars* are ±1 SEM. Statistically significant difference: ***$P < 0.001$. (**B**) The relationship between the reciprocal of near stereopsis and the absolute value of the postoperative CSR. Higher values on the x-axis indicate less nasotemporal balance of crowding effects after strabismus surgery, and higher values on the y-axis indicate better stereopsis. *Statistically significant linear correlation ($P < 0.05$).

Nasotemporal Rebalance in Visual Crowding Effects After Axial Alignment

Our results found peripheral visual crowding exhibited nasotemporal asymmetry in strabismic individuals but diminished and rebalanced after ocular alignment. To better characterize the surprising change of hemifield-specific crowding effects in older children and adults with strabismus, we calculated the ratio of the NCS between the nasal and the temporal hemifields (or CSR; see Methods). On average, the CSR was −0.14 ± 0.02 (mean ± SEM) at the radial axis and −0.12 ± 0.06 at the tangential axis for exotropes, as well as 0.13 ± 0.03 and 0.03 ± 0.04, respectively, for esotropes before surgery. After axial alignment, the corresponding value was −0.03 ± 0.04 and −0.01 ± 0.04 for exotropes and 0.01 ± 0.03 and 0.05 ± 0.04 for esotropes. In the exotropia group, the effect of surgical operation ($F_{1,\ 8} = 6.35$; $P = 0.029$) was significant, but the effect of the axis was not significant ($F_{1,\ 8} = 0.68$; $P = 0.427$) when a repeated-measures ANOVA was performed. A pairwise post hoc comparison (with Bonferroni correction) showed that the absolute value of the CSR for exotropes after surgery was significantly smaller than that before surgery along the radial axis (by 0.12, $t = -2.31$, $P = 0.042$). In the esotropia group, a repeated-measures ANOVA revealed that the effect of the interaction between surgical operation and axis was significant ($F_{1,\ 13} = 13.17$; $P = 0.003$), with a pairwise post hoc comparison (with Bonferroni correction) showing that the absolute value of the CSR after surgery was significantly smaller than that before surgery along the radial axis (by 0.12, $t = -2.92$, $P = 0.011$; Fig. 5). Moreover, a single-sample *t*-test showed that the CSR at the radial axis was significantly different from zero for both groups before surgery (EXO: $t = -6.39$, $P < 0.001$; ESO: $t = 4.22$, $P < 0.001$) but not

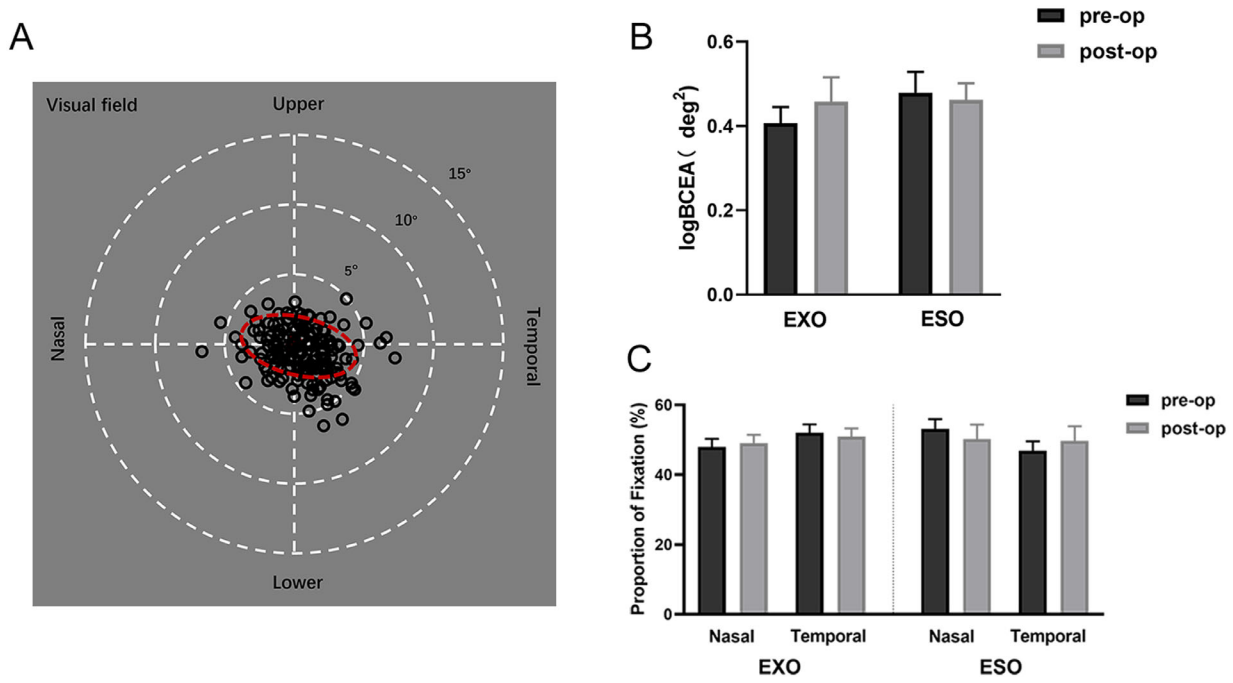

Figure 7. (**A**) Representation of the fixation on the visual field of a representative individual with the plot of the BCEA covering 68% of the fixation points. (**B**) Comparisons of the logBCEA of exotropia and esotropia groups before and after surgery. Higher values on the y-axis signify worse fixation stability. *Error bars* are ±1 SEM. (**C**) Comparisons of the proportion of fixation points between the nasal and temporal hemifields, as well as before and after surgery in different groups. Higher values on the y-axis signify greater fixation tendency. *Error bars* are ±1 SEM.

after surgery (EXO: $t = -0.88$, $P = 0.398$; ESO: $t = 0.37$, $P = 0.719$). However, no significant difference in the CSR from zero was found at the tangential axis for both groups regardless of surgery (all $P > 0.05$).

Correlations Between the CSR and Recovery of Stereopsis After Axial Alignment

Due to long-term ocular misalignment, most of our individuals had a loss of stereopsis. About 3 months after surgical correction, we found that 15 strabismic individuals (out of 27) partly recovered their near stereopsis. Since the change of the CSR was mainly exhibited in the radial axis, we compared the preoperative CSR at the radial axis between the individuals who manifested postoperative stereopsis recovery ($n = 15$) and individuals who did not ($n = 12$). The results showed that the absolute value of preoperative CSR of individuals with postoperative stereopsis recovery was significantly smaller than that of individuals without postoperative stereopsis recovery ($t = 4.22$, $P < 0.001$; Fig. 6A), indicating that severer preoperative nasoemporal asymmetry of visual crowding effects may predict poorer postoperative stereopsis recovery. We further analyzed the correlation between the stereopsis of individuals with postoperative stereopsis recovery and their corresponding postoperative CSR at the radial axis and found that there was a significant negative correlation between the reciprocal of near stereopsis and the absolute value of postoperative CSR ($r = -0.55$, $P = 0.034$; Fig. 6B). In other words, the more balanced the crowding effects between the nasal and temporal hemifields after surgery (i.e., the absolute value of the CSR approaching 0), the better the postoperative stereopsis of the individual.

Fixation Stability and Nasotemporal Bias of Fixation Eye Movements Before and After Surgical Alignment

Some studies have reported increased fixation instability in patients with strabismus.[9,49,51,52] To figure out whether strabismus surgery can improve the patient's fixation stability and thus reduce the visual crowding effects, we calculated and compared the logBCEA (deg^2) of individuals before and after surgical operation. There was no significant difference in the logBCEA before and after surgery for both exotropia (preoperative: 0.41 ± 0.13 vs. postoperative: 0.46 ± 0.20; $t = 0.73$, $P = 0.47$, two-tailed paired samples *t*-test) and esotropia groups (preoperative: 0.48 ± 0.19 vs. postoperative: 0.46 ± 0.15; $t = 0.27$, $P = 0.79$; Fig. 7B). We further analyzed the distribution of fixation points in the nasal and temporal visual fields during the test to eliminate the influence of oculomotor bias on the crowding effects detection. The results showed that the proportion of fixation points in the nasal and temporal hemifields was roughly similar and symmetrical whether before or after the operation (all $P > 0.05$, two-tailed paired samples *t*-test; Fig. 7C).

Discussion

In the current study, secured by a real-time eye tracker to fulfill gaze-contingent display, we found that optical realignment (i.e., strabismus surgery) could normalize the enlarged visual crowding effects, a reliable psychophysical index of cortical organization, in the peripheral visual field of older children and adults with strabismus and rebalance the nasotemporal asymmetry of crowding along the radial axis, promoting the recovery of postoperative stereopsis.

Our results indicated a potential of experience-dependent cortical organization after axial alignment even for older children and adults who are out of the critical period of visual development.

Previous neurophysiologic and brain imaging studies have suggested that crowding is a cortical phenomenon and may originate in the early visual cortex (i.e., V1), with its perceptual consequence influenced by the downstream visual areas (i.e., V2, V3, V4, or higher-level visual areas).[14,22,24,53,54] In this study, we observed a hemifield- and radial- specific reduction of crowding effects across the visual fields after strabismus surgery. This kind of anisotropic change in the crowding effects is consistent with the horizontal deviation of the eye, and we postulate that this may be due to plasticity at the cortical level.[32,55] The transition to adulthood entails a reduction in the plastic potential of the visual cortex.[56,57] However, growing experimental studies in animal models and humans have shown that physiologic plasticity can be enabled in the adult cortex as well.[58,59] By selecting a group of older children and adults with long-term strabismus history and relatively large angles of misalignment, our findings suggest that the visual system of adulthood is still capable of reorganizing its sensory coding to adapt to improved visual input. Besides, previous studies have revealed that perceptual learning can reduce crowding effects in the normal periphery, which also imply an experience-dependent plasticity on the cortical substrates of crowding.[16,22,27] On these bases, we think strabismus surgery is more than a cosmetic surgery but also can improve visual functions even in adulthood.[60,61] We do not attribute these improvements to patients' learning effect of the test task, because first, no feedback was given to patients during the test, and thus it was not so easy to have learning effects. Second, there was an interval of about 3 months between preoperative and postoperative measurement. Third, in our previous study,[33] we have retested the normal control group at the same interval and found that the results were similar and far lower than the improvement of surgery (see Supplementary Fig. S1).

Although some studies have suggested an increased fixation instability in patients with strabismus as well as nasotemporal bias for motion and perception,[9,62–64] our results of fixation eye movements showed relatively stable fixation stability and nasaotemporal symmetrical fixation before and after strabismus surgery. We also excluded individuals with clinical nystagmus who are proved to be more fixation unstable and less likely to have recovery of stereopsis.[49] Thus, we also do not attribute the features and improvements of crowding effects to patients' changes in fixation eye movements.

What is interesting is that we found a correlation between the restored stereopsis and the extent of nasotemporal balance of crowding effects, indicating adult brain plasticity and signifying the importance of ocular correction. We speculate that the rebalanced binocular input after axial alignment may be conducive to the restoration and improvement of binocular visual functions. It is uncovered that better binocular outcomes are obtained when interocular imbalance is corrected after surgical correction,[65,66] and microstructural changes of visuospatial network tracts may be the reason.[32] Whereas stereopsis is one of the key indicators for evaluating visual functions and plays an important role in daily work and life,[3] our results suggest that assessment of visual crowding across visual fields has important implications for clinical practice to provide a more comprehensive evaluation of visual functions before and after surgical correction in strabismus, as well as for our understanding of peripheral vision and object recognition.

There were some limitations of the current study. First, our study included a relatively small sample of patients and a follow-up for only 3 months. Additional investigations with larger samples and followed up by a longitudinal study are needed to help further elucidate the surgical outcomes of crowding effects and other clinical improvements of strabismus. In addition, although our results revealed the functional change of peripheral visual crowding effects of strabismic individuals, the substrate of cortical processing in object recognition following long-term adaptation to ocular deviation as well as axis realignment remains unclear, which merits further examination in future neuroimaging and electrophysiology researches.

In conclusion, we measured visual crowding, an essential bottleneck on object recognition and a reliable psychophysical index of cortex organization, in older children and adults with strabismus before and after strabismus surgery. We found that the peripheral visual crowding was reduced and became rebalanced between the nasal and temporal hemifields after surgery, associating with a recovery of postoperative stereopsis. Our results indicated strong experience-dependent cortical reorganization after axial alignment and signify the importance of ocular correction for clinical practice.

Acknowledgments

Supported by the Natural Science Foundation of China Grant NSFC 82271115 (MY), Guangdong Basic and Applied Basic Research Foundation (2023A1515011829) (ZL), Natural Science Foundation of China Grant NSFC 32100864 (F-FY), and Natural Science Foundation of China Grant NSFC 32071056 (C-BH).

Disclosure: **Y. Huang**, None; **Z. Liu**, None; **M. Wang**, None; **L. Gao**, None; **Y. Wu**, None; **J. Hu**, None; **Z. Zhang**, None; **F.-F. Yan**, None; **D. Deng**, None; **C.-B. Huang**, None; **M. Yu**, None

References

1. Tan L, Ringach DL, Zipursky SL, Trachtenberg JT. Vision is required for the formation of binocular neurons prior to the classical critical period. *Curr Biol*. 2021;31:4305–4313.e5.
2. Ishikawa AW, Komatsu Y, Yoshimura Y. Experience-dependent development of feature-selective synchronization in the primary visual cortex. *J Neurosci*. 2018;38:7852–7869.
3. Birch EE. Amblyopia and binocular vision. *Prog Retin Eye Res*. 2013;33:67–84.
4. Hashemi H, Pakzad R, Heydarian S, et al. Global and regional prevalence of strabismus: a comprehensive systematic review and meta-analysis. *Strabismus*. 2019;27:54–65.
5. Liu L-Q, Li Q-Y, Zhang Z-H, et al. Altered functional connectivity of primary visual cortex in adults with strabismus and amblyopia: a resting-state fMRI study. *J Integr Neurosci*. 2022;21:4.
6. Guo Y, Fu J, Hong J, Liu Z, He X. Functional changes in the visual cortex in preoperative and postoperative patients with intermittent exotropia: study protocol for a non-randomised case-control clinical trial. *BMJ Open*. 2022;12:e055848.
7. Yan X, Wang Y, Xu L, et al. Altered functional connectivity of the primary visual cortex in adult comitant strabismus:

a resting-state functional MRI study. *Curr Eye Res*. 2019; 44:316–323.
8. Buffenn AN. The impact of strabismus on psychosocial heath and quality of life: a systematic review. *Surv Ophthalmol*. 2021;66:1051–1064.
9. Ghasia FF, Otero-Millan J, Shaikh AG. Abnormal fixational eye movements in strabismus. *Br J Ophthalmol*. 2018;102:253–259.
10. Sawamura H, Gillebert CR, Todd JT, Orban GA. Binocular stereo acuity affects monocular three-dimensional shape perception in patients with strabismus. *Br J Ophthalmol*. 2018;102:1413–1418.
11. Donahue SP. Clinical practice. Pediatric strabismus. *N Engl J Med*. 2007;356:1040–1047.
12. Manassi M, Whitney D. Multi-level crowding and the paradox of object recognition in clutter. *Curr Biol*. 2018;28:R127–R133.
13. Grainger J, Dufau S, Ziegler JC. A vision of reading. *Trends Cogn Sci*. 2016;20:171–179.
14. Whitney D, Levi DM. Visual crowding: a fundamental limit on conscious perception and object recognition. *Trends Cogn Sci*. 2011;15:160–168.
15. Pelli DG. Crowding: a cortical constraint on object recognition. *Curr Opin Neurobiol*. 2008;18:445–451.
16. Malania M, Pawellek M, Plank T, Greenlee MW. Training-induced changes in radial-tangential anisotropy of visual crowding. *Transl Vis Sci Technol*. 2020;9:25.
17. Chung STL. Cortical reorganization after long-term adaptation to retinal lesions in humans. *J Neurosci*. 2013;33:18080–18086.
18. Toet A, Levi DM. The two-dimensional shape of spatial interaction zones in the parafovea. *Vis Res*. 1992;32:1349–1357.
19. Bouma H. Interaction effects in parafoveal letter recognition. *Nature*. 1970;226:177–178.
20. Rosenholtz R. Capabilities and limitations of peripheral vision. *Annu Rev Vis Sci*. 2016;2:437–457.
21. Kwon M, Liu R. Linkage between retinal ganglion cell density and the nonuniform spatial integration across the visual field. *Proc Natl Acad Sci USA*. 2019;116:3827–3836.
22. He D, Wang Y, Fang F. The critical role of V2 population receptive fields in visual orientation crowding. *Curr Biol*. 2019;29:2229–2236.e3.
23. Chen J, He Y, Zhu Z, et al. Attention-dependent early cortical suppression contributes to crowding. *J Neurosci*. 2014;34:10465–10474.
24. Levi DM. Crowding—an essential bottleneck for object recognition: a mini-review. *Vis Res*. 2008;48:635–654.
25. Shamsi F, Liu R, Kwon M. Foveal crowding appears to be robust to normal aging and glaucoma unlike parafoveal and peripheral crowding. *J Vis*. 2022;22:10.
26. Ogata NG, Boer ER, Daga FB, Jammal AA, Stringham JM, Medeiros FA. Visual crowding in glaucoma. *Invest Ophthalmol Vis Sci*. 2019;60:538–543.
27. Hussain Z, Webb BS, Astle AT, McGraw PV. Perceptual learning reduces crowding in amblyopia and in the normal periphery. *J Neurosci*. 2012;32:474–480.
28. Berry KP, Nedivi E. Experience-dependent structural plasticity in the visual system. *Annu Rev Vis Sci*. 2016;2:17–35.
29. Edelman PM. Functional benefits of adult strabismus surgery. *Am Orthopt J*. 2010;60:43–47.
30. Murray ADN, Orpen J, Calcutt C. Changes in the functional binocular status of older children and adults with previously untreated infantile esotropia following late surgical realignment. *J AAPOS*. 2007;11:125–130.
31. Kushner BJ, Morton GV. Postoperative binocularity in adults with longstanding strabismus. *Ophthalmology*. 1992;99:316–319.
32. Wang Y, Wang X, Shi H, et al. Microstructural properties of major white matter tracts in constant exotropia before and after strabismus surgery. *Br J Ophthalmol*. 2021;106:870–877.
33. Huang Y, Liu Z, Chen Z, et al. Visual crowding reveals field- and axis-specific cortical miswiring after long-term axial misalignment in strabismic patients without amblyopia. *Invest Ophthalmol Vis Sci*. 2023;64:10.
34. Dagi LR, Velez FG, Archer SM, et al. Adult strabismus preferred practice pattern. *Ophthalmology*. 2020;127:P182–P298.
35. Tang SM, Chan RYT, Bin Lin S, et al. Refractive errors and concomitant strabismus: a systematic review and meta-analysis. *Sci Rep*. 2016;6:35177.
36. Burian H. Horizontal concomitant strabismus. *Am J Ophthalmol*. 1951;34:908.
37. Wallace DK, Christiansen SP, Sprunger DT, et al. Esotropia and exotropia preferred practice pattern. *Ophthalmology*. 2018;125:P143–P183.
38. Brainard DH. The Psychophysics Toolbox. *Spat Vis*. 1997;10:433–436.
39. Kwon M, Nandy AS, Tjan BS. Rapid and persistent adaptability of human oculomotor control in response to simulated central vision loss. *Curr Biol*. 2013;23:1663–1669.
40. Chung ST, Levi DM, Legge GE. Spatial-frequency and contrast properties of crowding. *Vis Res*. 2001;41:1833–1850.
41. Rombouts SA, Barkhof F, Sprenger M, Valk J, Scheltens P. The functional basis of ocular dominance: functional MRI (fMRI) findings. *Neurosci Lett*. 1996;221:1–4.
42. Miles WR. Ocular dominance in human adults. *J Gen Psychol*. 1929;3:412–430.
43. Harrar V, Le Trung W, Malienko A, Khan AZ. A nonvisual eye tracker calibration method for video-based tracking. *J Vis*. 2018;18:13.
44. Cornsweet TN. The staircase-method in psychophysics. *Am J Psychol*. 1962;75:485–491.
45. Levitt H. Transformed up-down methods in psychoacoustics. *J Acoust Soc Am*. 1971;49(suppl 2):467+.
46. Greenwood JA, Szinte M, Sayim B, Cavanagh P. Variations in crowding, saccadic precision, and spatial localization reveal the shared topology of spatial vision. *Proc Natl Acad Sci USA*. 2017;114:E3573–E3582.
47. Petrov Y, Meleshkevich O. Asymmetries and idiosyncratic hot spots in crowding. *Vis Res*. 2011;51:1117–1123.
48. Altemir I, Alejandre A, Fanlo-Zarazaga A, et al. Evaluation of fixational behavior throughout life. *Brain Sci*. 2021;12:19.
49. Martin TL, Murray J, Garg K, Gallagher C, Shaikh AG, Ghasia FF. Fixation eye movement abnormalities and stereopsis recovery following strabismus repair. *Sci Rep*. 2021;11:14417.
50. Murray J, Gupta P, Dulaney C, Garg K, Shaikh AG, Ghasia FF. Effect of viewing conditions on fixation eye movements and eye alignment in amblyopia. *Invest Ophthalmol Vis Sci*. 2022;63:33.
51. Economides JR, Adams DL, Horton JC. Variability of ocular deviation in strabismus. *JAMA Ophthalmol*. 2016;134:63–69.
52. Ciuffreda KJ, Kenyon RV, Stark L. Saccadic intrusions in strabismus. *Arch Ophthalmol*. 1979;97:1673–1679.
53. Chen N, Bao P, Tjan BS. Contextual-dependent attention effect on crowded orientation signals in human visual cortex. *J Neurosci*. 2018;38:8433–8440.
54. Anderson EJ, Dakin SC, Schwarzkopf DS, Rees G, Greenwood JA. The neural correlates of crowding-induced changes in appearance. *Curr Biol*. 2012;22:1199–1206.
55. Chen N, Shin K, Millin R, Song Y, Kwon M, Tjan BS. Cortical reorganization of peripheral vision induced by simulated central vision loss. *J Neurosci*. 2019;39:3529–3536.

Investigative Ophthalmology & Visual Science

56. Baroncelli L, Lunghi C. Neuroplasticity of the visual cortex: in sickness and in health. *Exp Neurol*. 2021;335:113515.
57. Hooks BM, Chen C. Critical periods in the visual system: changing views for a model of experience-dependent plasticity. *Neuron*. 2007;56:312–326.
58. Hooks BM, Chen C. Circuitry underlying experience-dependent plasticity in the mouse visual system. *Neuron*. 2020;106:21–36.
59. Siu CR, Beshara SP, Jones DG, Murphy KM. Development of glutamatergic proteins in human visual cortex across the lifespan. *J Neurosci*. 2017;37:6031–6042.
60. Estes KJ, Parrish RK, Sinacore J, Mumby PB, McDonnell JF. Effects of corrective strabismus surgery on social anxiety and self-consciousness in adults. *J AAPOS*. 2020;24:280.e281–280.e284.
61. Gunton KB. Impact of strabismus surgery on health-related quality of life in adults. *Curr Opin Ophthalmol*. 2014;25:406–410.
62. Kelly KR, Cheng-Patel CS, Jost RM, Wang Y-Z, Birch EE. Fixation instability during binocular viewing in anisometropic and strabismic children. *Exp Eye Res*. 2019;183:29–37.
63. Hussain Z, Astle AT, Webb BS, McGraw PV. Position matching between the visual fields in strabismus. *J Vis*. 2018;18:9.
64. Economides JR, Adams DL, Horton JC. Perception via the deviated eye in strabismus. *J Neurosci*. 2012;32:10286–10295.
65. Zhou J, Wang Y, Feng L, Wang J, Hess RF. Straightening the eyes doesn't rebalance the brain. *Front Hum Neurosci*. 2017;11:453.
66. Feng L, Zhou J, Chen L, Hess RF. Sensory eye balance in surgically corrected intermittent exotropes with normal stereopsis. *Sci Rep*. 2015;5:13075.